A weighted particle scheme for solving the Enskog-Vlasov equation in spherical geometry

Sergiu Busuioc

Department of Physics, West University of Timişoara, 300223 Timişoara, Romania

29 of August 2022

Motivation

The aim of this research is to develop a weighted particle scheme for solving the Enskog-Vlasov equation in spherical geometry. This required a special treatment of the collision mechanism as well as an efficient way to evaluate the mean-field in spherical coordinates. As test problems for the new numerical scheme we've chosen the growth of droplets/bubbles in metastable vapor/liquid.

Introduction

Let us consider a fluid composed of identical spherical atoms of mass m and diameter a interacting through the Sutherland potential defined by the superposition of the hard sphere potential and an algebraic attractive soft potential tail:

$$\phi(\rho) = \begin{cases} +\infty\,, & \rho < a, \\ -\phi_a \left(\dfrac{\rho}{a}\right)^{-\gamma}, & \rho \geq a, \end{cases} \tag{1}$$

where $\rho = ||\boldsymbol{r}_1 - \boldsymbol{r}_2||$ is the distance between the interacting atoms at position $\boldsymbol{r}_1$ and $\boldsymbol{r}_2$, and the two positive constants ϕ_a and γ define the depth of the potential well and the range of the soft interaction, respectively.

Introduction

The evolution equation of the one-particle distribution in spherically symmetric systems reads:

$$\frac{\partial f}{\partial t} + v_r \frac{\partial f}{\partial r} + \left(\frac{\mathcal{F}_r[n]}{m} - \frac{v_t^2}{r} \right) \frac{\partial f}{\partial v_r} = \mathcal{C}_E[f], \tag{2}$$

where $\mathcal{F}_r[n]$ is the radial component of the self-consistent force field generated by the soft attractive tail, which depends on the number density field $n(r,t)$, and $\mathcal{C}_E[f]$ is the hard-sphere collision integral (square brackets are used to highlight the functional dependence).

Collision integral

The hard-sphere collision integral is given by:

$$\mathcal{C}_E[f] = a^2 \int d\boldsymbol{v}_1 d^2\hat{\boldsymbol{k}}\, (\boldsymbol{v}_{rel}\cdot\hat{\boldsymbol{k}})^+ \left\{ \chi\left[n\left(r\hat{\boldsymbol{r}} + \frac{a}{2}\hat{\boldsymbol{k}}, t\right)\right] f(r\hat{\boldsymbol{r}} + a\hat{\boldsymbol{k}}, \boldsymbol{v}_1', t) f(r, \boldsymbol{v}', t) \right.$$
$$\left. - \chi\left[n\left(r\hat{\boldsymbol{r}} - \frac{a}{2}\hat{\boldsymbol{k}}, t\right)\right] f(r\hat{\boldsymbol{r}} - a\hat{\boldsymbol{k}}, \boldsymbol{v}_1, t) f(r, \boldsymbol{v}, t) \right\}, \quad (3)$$

where $(\cdot)^+$ indicates that the surface integral is restricted to the half-sphere for which $\boldsymbol{v}_{rel}\cdot\hat{\boldsymbol{k}} > 0$, $\hat{\boldsymbol{r}}$ is the unit vector in the radial direction, and $\chi[n]$ is the contact value of the pair correlation function in a hard-sphere fluid in equilibrium with number density n[1]. The pair correlation function is approximated as in standard Enskog theory (SET), and the Fischer-Methfessel approach[2] is used to evaluate the density at the contact point of the colliding atoms, namely:

$$\chi\left[n\left(r\hat{\boldsymbol{r}} \pm \frac{a}{2}\hat{\boldsymbol{k}}, t\right)\right] = \chi_{\text{SET}}\left(\overline{n}\left(r\hat{\boldsymbol{r}} \pm \frac{a}{2}\hat{\boldsymbol{k}}\right)\right) = \frac{1}{2}\frac{2-\eta}{(1-\eta)^3}, \qquad \eta = \frac{\pi a^3 \overline{n}}{6}. \quad (4)$$

[1] G. M. Kremer, Springer-Verlag, Berlin Heidelberg, 2010

[2] J. Fischer, M. Methfessel, Phys. Rev. A 22 (6) (1980) 2836

Self-consistent force field - Illustration

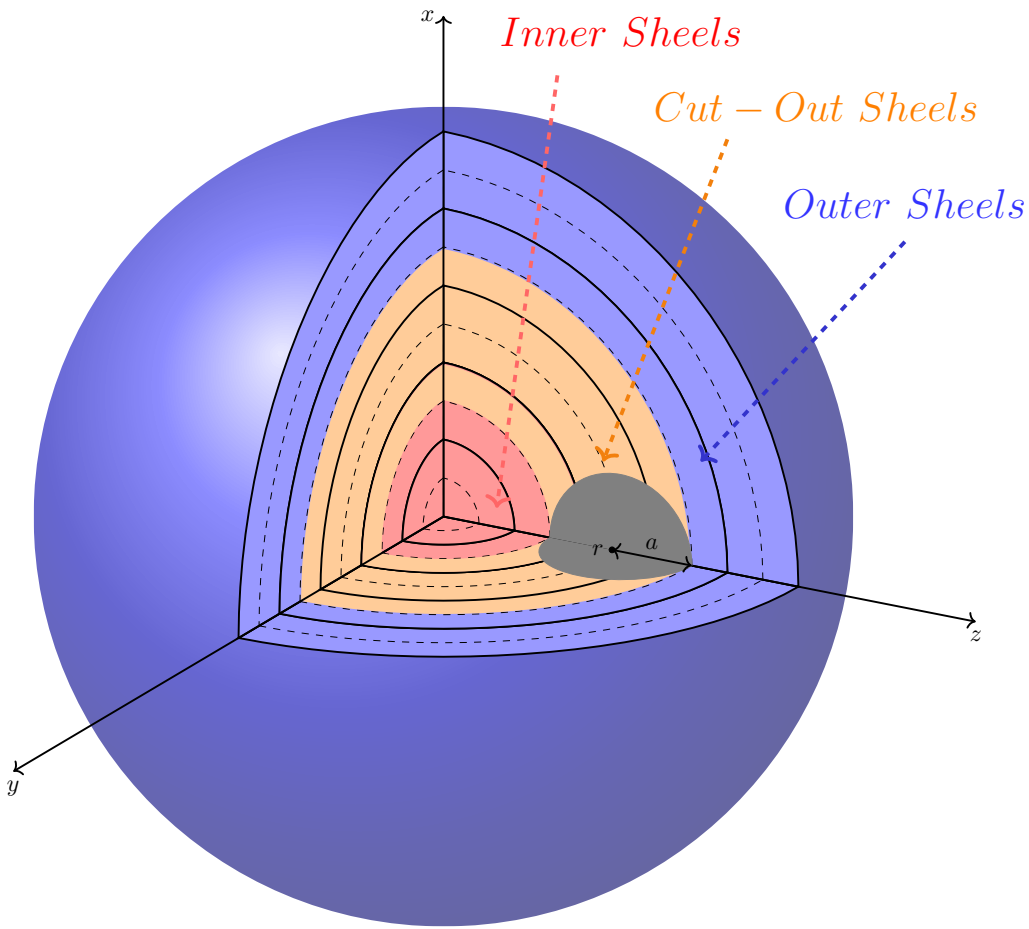

Figure: Radial component of the self-consistent force field evaluation. The spherical shells are partitioned into 3 groups: the inner shells, the outer shells and the cutout spherical shells .The cut out sphere of radius a has the origin on the cell center and, subsequently, the edges on a cell center.

Self-consistent force field - Evaluation

The general expression of the self-consistent force field generated by the soft attractive tail is given by:

$$\mathcal{F}[n] = \int_{||\boldsymbol{r}_1 - \boldsymbol{r}|| > a} \frac{d\phi_a(\rho)}{d\rho} \frac{\boldsymbol{r}_1 - \boldsymbol{r}}{||\boldsymbol{r}_1 - \boldsymbol{r}||} n(\boldsymbol{r_1}) d\boldsymbol{r_1}. \tag{5}$$

The radial component of the self-consistent force field obtained for $\gamma = 6$:

$$\mathcal{F}_r[n(r,t)] = 2\pi\phi_a a^6 \left[\int_{|r-R|>a} \frac{4(3r^3R^2 + 5rR^4)n(R,t)}{(R-r)^5(R+r)^5} dR \right.$$
$$\left. + \int_{|r-R|\leq a} \frac{R}{4r^2} \left(\frac{3}{a^4} + \frac{2(R-r)(R+r)}{a^6} - \frac{5r+R}{(R+r)^5} \right) n(R,t) dR \right] \tag{6}$$

Numerical scheme - Streaming algorithm

Variables: N_p: total number of particles; $w_{i/j}$: weight of particle i and j;
for $i = 1$ **to** N_p **do**
    Compute the half-step radial velocity component;
    Compute the new radial position;
    Evaluate the mean force field;
    Bring the velocity components back to the radial axis;
    Update the radial velocity component to full time step;
    Identify the cell j occupied by particle i;
    if $(w_i > w_j)$ **then**
        Update the weight of particle i to w_j;
        Create $[w_i/w_j] - 1$ copies of weight w_j;
        Create an additional copy of weight w_j with probability:
        $w_i/w_j - [w_i/w_j]$;
    else
        Delete particle i;
        Create a particle of weight w_j with probability w_i/w_j;
    end
end

Collision process

The probabilistic rule for updating the velocity of the colliding pair is to assume that the particle with lower weight always changes its velocity, whereas the particle with larger weight does it with a probability equal to the ratio of the two weights [3]:

$$\boldsymbol{v}_i' = \boldsymbol{v}_i + (\boldsymbol{v}_r \cdot \hat{\boldsymbol{k}})\boldsymbol{v}_i' \quad \text{with probability} \quad \frac{\min(w_i, w_j)}{w_i}, \tag{7}$$

$$\boldsymbol{v}_j' = \boldsymbol{v}_j - (\boldsymbol{v}_r \cdot \hat{\boldsymbol{k}})\boldsymbol{v}_i' \quad \text{with probability} \quad \frac{\min(w_i, w_j)}{w_j}. \tag{8}$$

[3] G. A. Bird, Molecular Gas Dynamics, Oxford Univ. Press, Oxford, England, UK, 1976

Collision process - Number of collisions

The key point is that two colliding weighted particles can be regarded as two molecular beams composed of w_i and w_j atoms. The expected number of collisions between atoms per unit time is thus given by:

$$N_c = w_i w_j \sigma_{ij} \tag{9}$$

where σ_{ij} is the total cross section of atoms.
As weighted particles are made to collide only in probability based on Eqs. (7), the expected average number of collisions is:

$$N_c = \frac{1}{2}\left(w_i w_j \sigma'_{ij} \frac{\min(w_i, w_j)}{w_i} + w_j w_i \sigma'_{ij} \frac{\min(w_i, w_j)}{w_j} \right) \tag{10}$$

where σ'_{ij} is the total collisional cross section of the weighted particles. By equating Eqs.(9) and (10), it follows that:

$$\sigma'_{ij} = \frac{2 w_i w_j}{(w_i + w_j)\min(w_i, w_j)} \sigma_{ij} = \frac{2\max(w_i, w_j)}{(w_i + w_j)} \sigma_{ij} \tag{11}$$

Collision process - Illustration

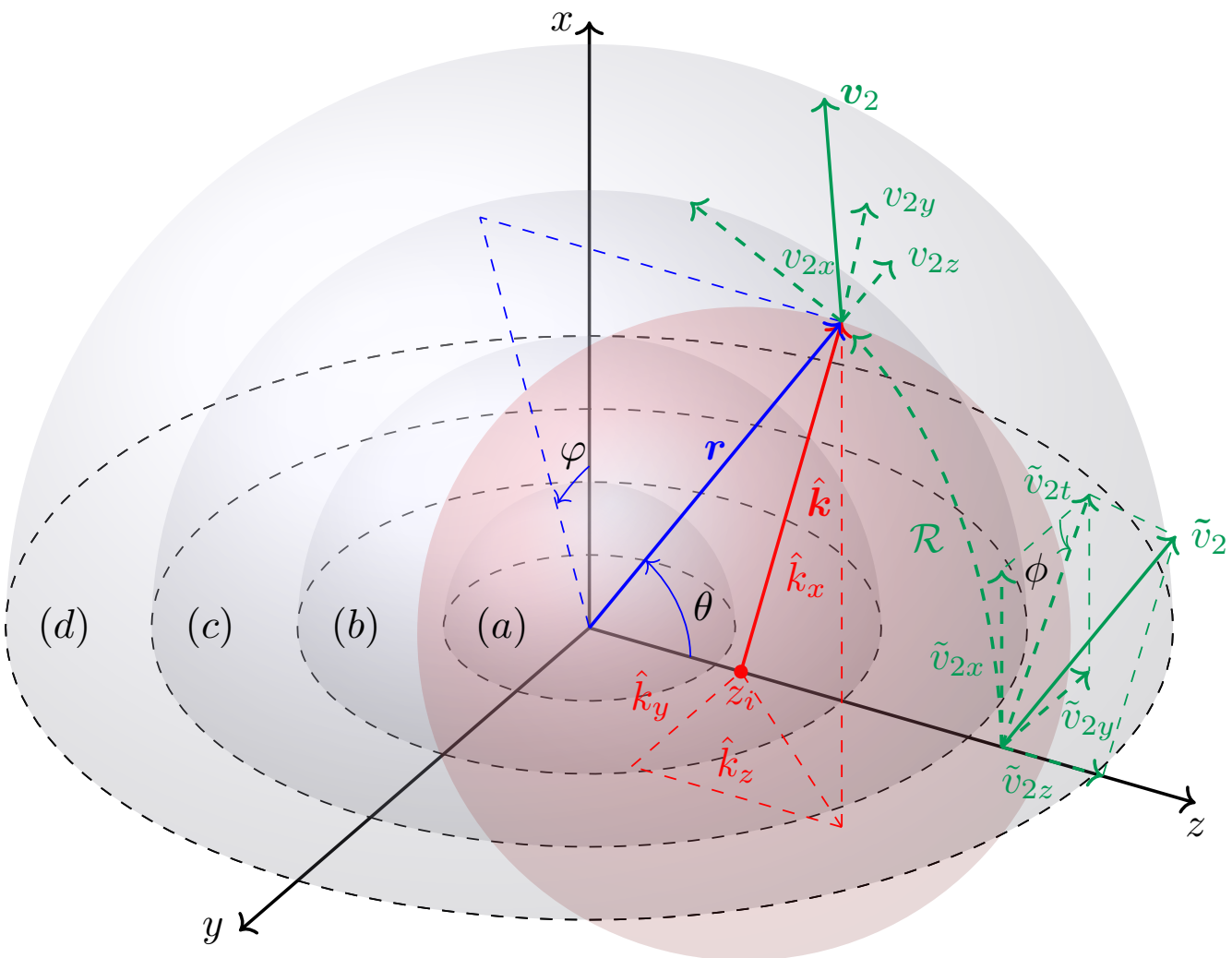

Collision partner selection. The radial axis is identified with the z axis.

Collision process - algorithm

Algorithm 1: Collision Step

Variables: N_c: total number of collisions;
$w_{i/j}$: weight of particle i and j

Evaluate N_c ;

for $ic = 1$ **to** N_c **do**

- Select a particle ;
- Generate a random unit vector $\hat{\boldsymbol{k}}$;
- Select the collision partner and rotate its velocity ;
- Evaluate the scalar product $\vec{\boldsymbol{v}_{rel}} \cdot \hat{\boldsymbol{k}}$;
- **if** $(\vec{\boldsymbol{v}_{rel}} \cdot \hat{\boldsymbol{k}}) > 0$ **and** *collision is real* **then**
  - update post-collisional vel. $\vec{\boldsymbol{v}_{\boldsymbol{i}}}'$ with probability $\min\{1; w_j/w_i\}$;
  - update post-collisional vel. $\vec{\boldsymbol{v}_{\boldsymbol{j}}}'$ with probability $\min\{1; w_i/w_j\}$;
  - rotate $\boldsymbol{v}_{\boldsymbol{j}}'$ back to the z-axis;
- **end**

end

Conservation

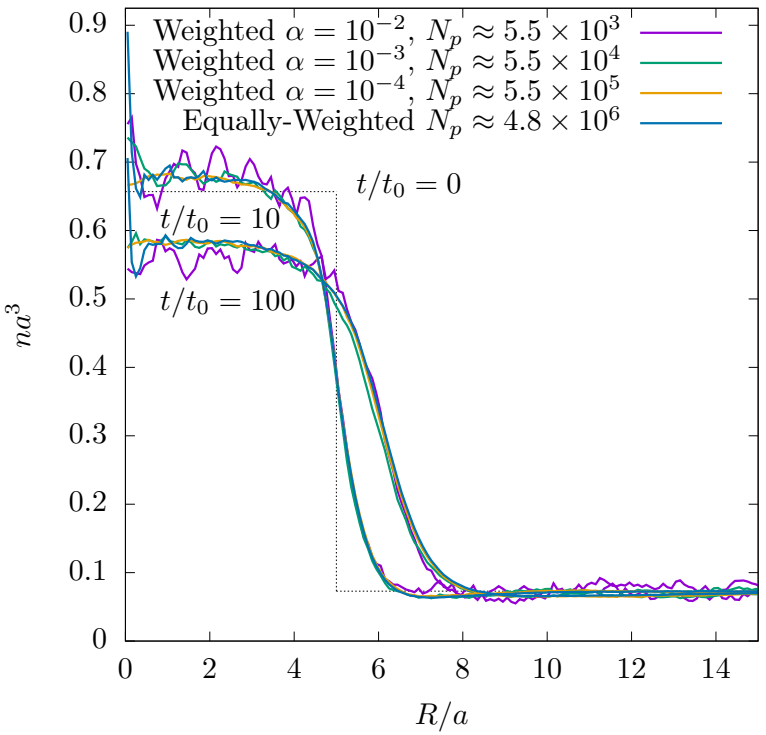

(a) Constant vs varying weights

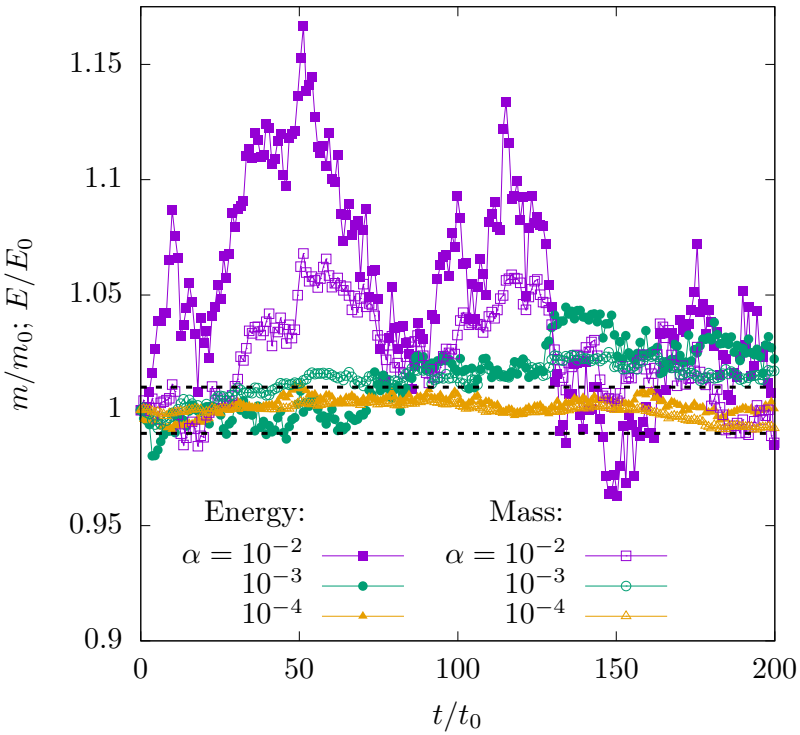

(b) Conservation properties

Figure: Validation case study I: Sample droplet growth simulation. (a) Comparison of runs with different number of simulation particles and constant/varying weights. (b) Time evolution of normalised total mass and total kinetic energy for different values of α; m_0 and E_0 represent the total initial mass and total kinetic energy, respectively.

Validation - Fluid surface tension

T/T_c	Planar[4]	Cylindrical[4]	Spherical
0.729	0.184	0.178	0.180
0.795	0.123	0.121	0.118
0.861	0.0698	0.0675	0.068

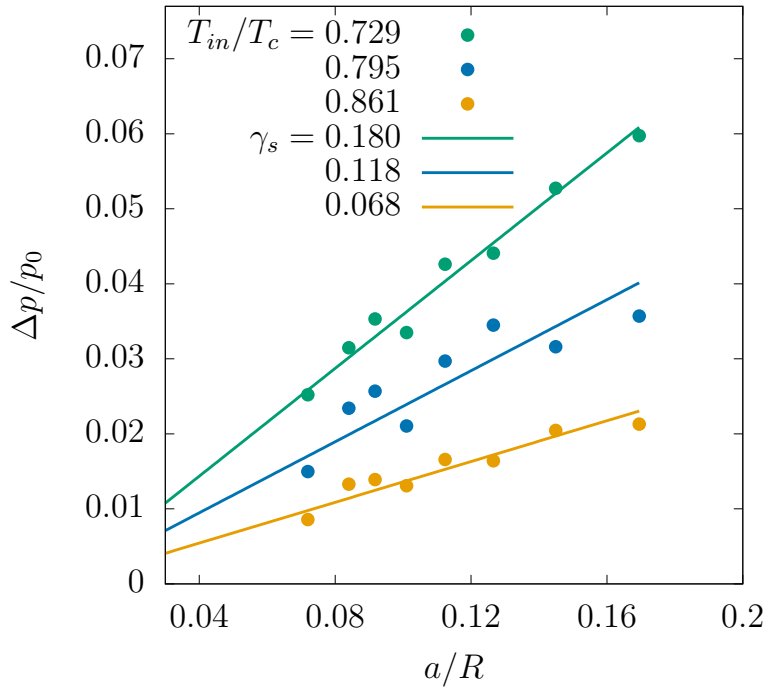

Figure: Validation case study I: Pressure difference at the liquid-vapor interface, $\Delta p/p_0$, versus the reciprocal of the droplet radius, a/R, for different temperatures.

[4] P. Barbante, A. Frezzotti, L. Gibelli, Kinet. Relat. Mod. 8 (2) (2015) 235–254.

Validation - Droplet critical radius

From the classical nucleation theory (CNT), the critical radius, R^*, is given by:

$$R^* = \frac{2\gamma_s}{n_\ell k_\mathrm{B} T \ln S} \tag{12}$$

where $S = p(T, n_v)/p(T)$ and n_ℓ is the eq. liquid density at the temperature T.

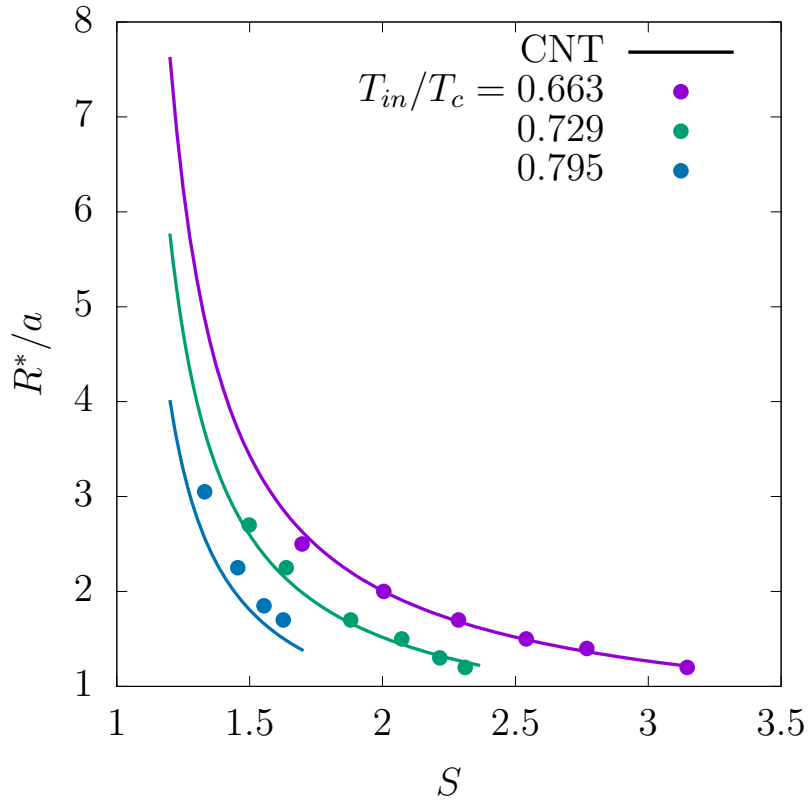

Figure: Dimensionless critical radius, R^*/a, versus the supersaturation ratio S for different values of the temperatures.

Phase diagram

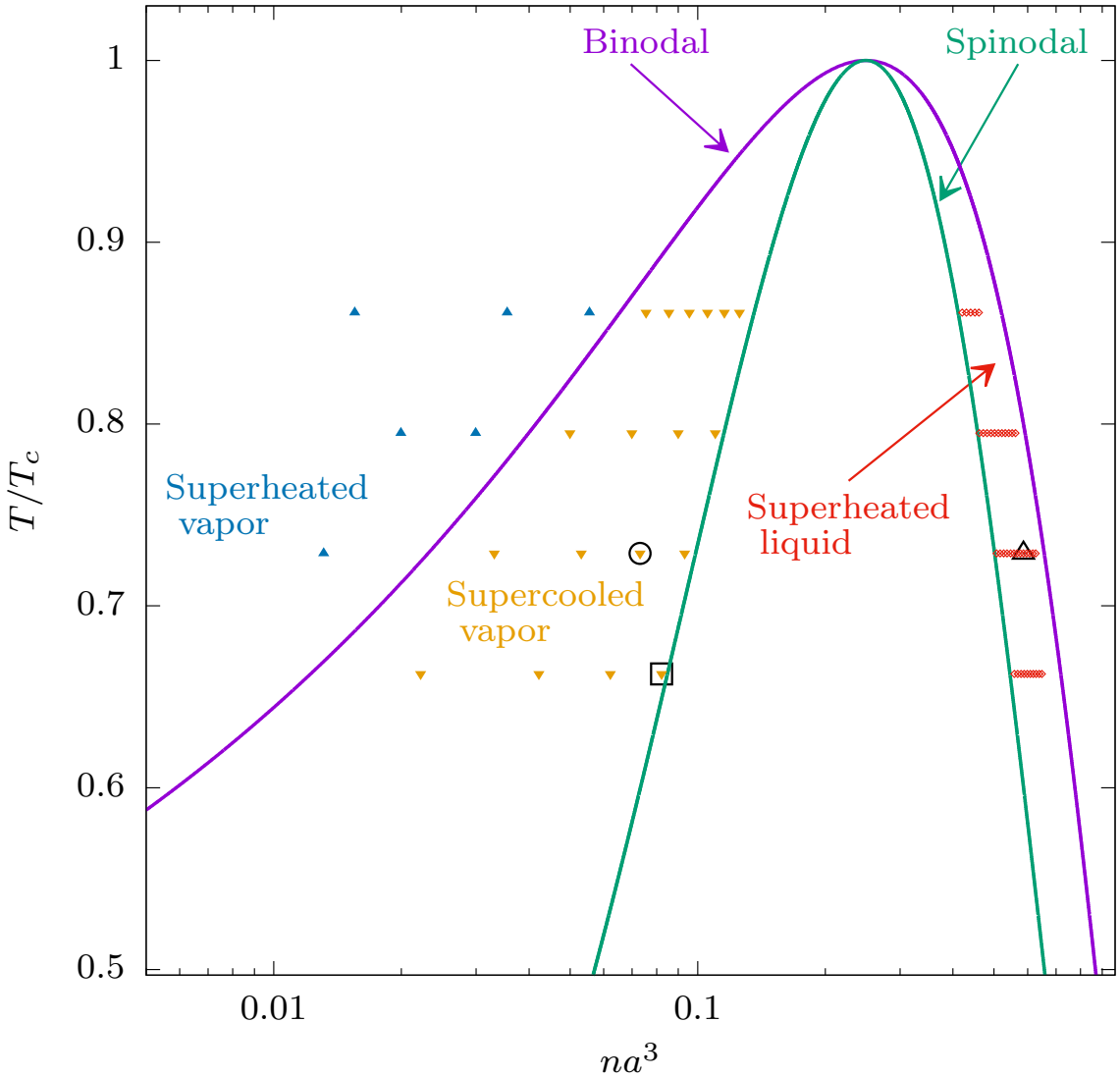

Phase diagram. Solid symbols represent the initial conditions of the simulation campaign carry out to evaluate the growth rate of droplets and bubbles.

Growth of liquid droplets in metastable vapor

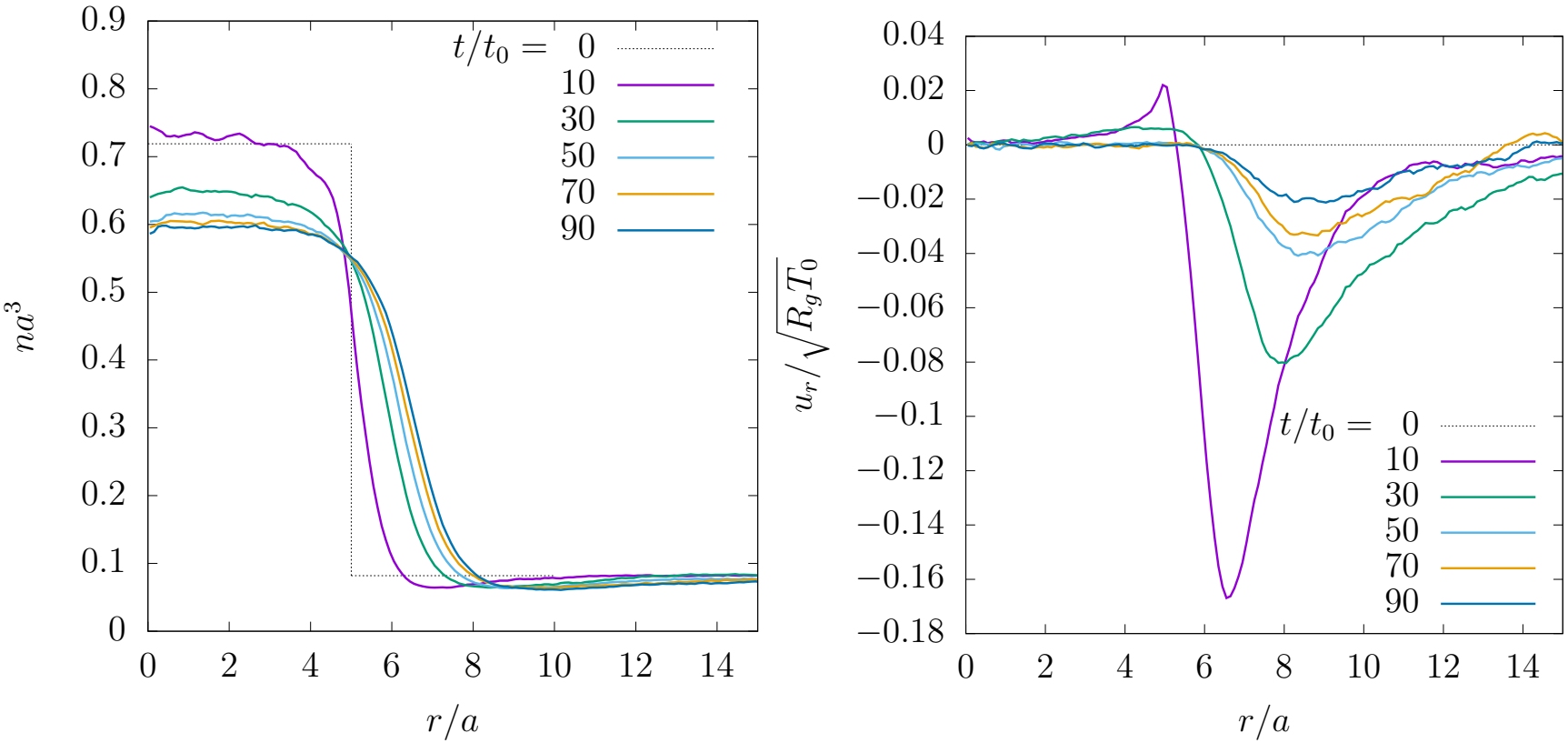

(a) Density: $T/T_c = 0.663, S = 3.67$

(b) u_r: $T/T_c = 0.663, S = 3.67$

Figure: (a) Density, (b) radial velocity (c) temperature profiles during droplet growth. Results corresponding to the case $T/T_c = 0.663$, $S = 3.67$. (d) Bulk droplet temperature time evolution at $T/T_c = 0.663$ and various values of the supercooling ratio S.

Growth of liquid droplets in metastable vapor

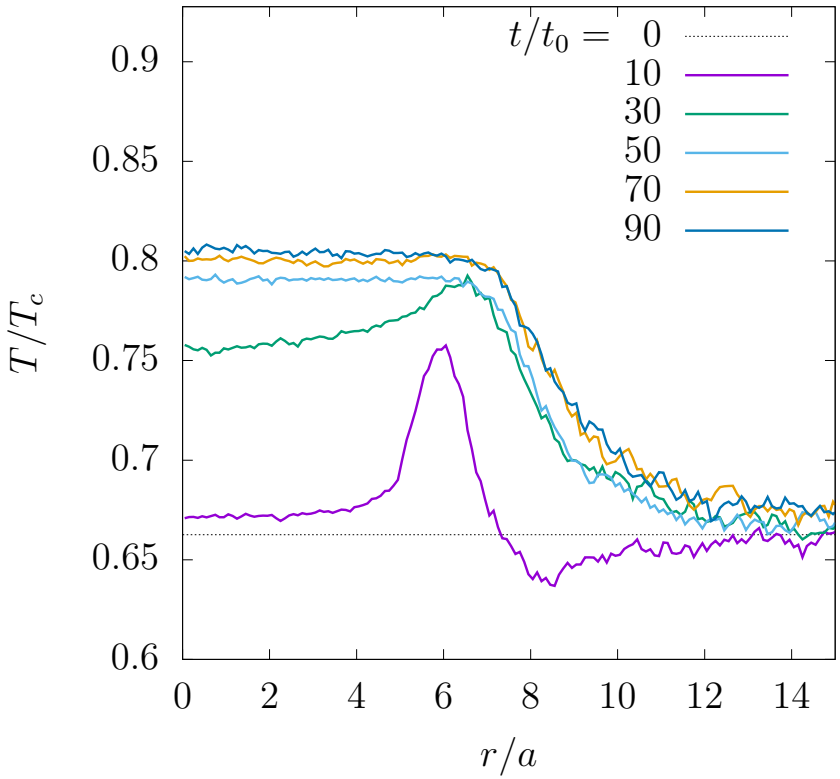

(a) Temperature: $T/T_c = 0.663, S = 3.67$

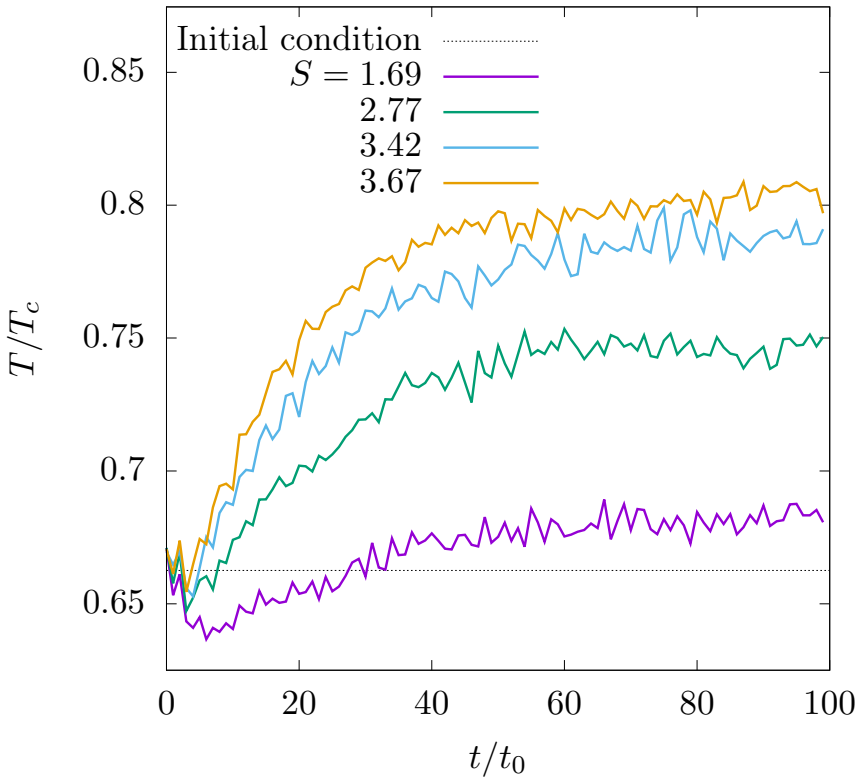

(b) Bulk liquid temperature evolution

Figure: (a) Density, (b) radial velocity (c) temperature profiles during droplet growth. Results corresponding to the case $T/T_c = 0.663$, $S = 3.67$. (d) Bulk droplet temperature time evolution at $T/T_c = 0.663$ and various values of the supercooling ratio S.

Growth of liquid droplets in metastable vapor

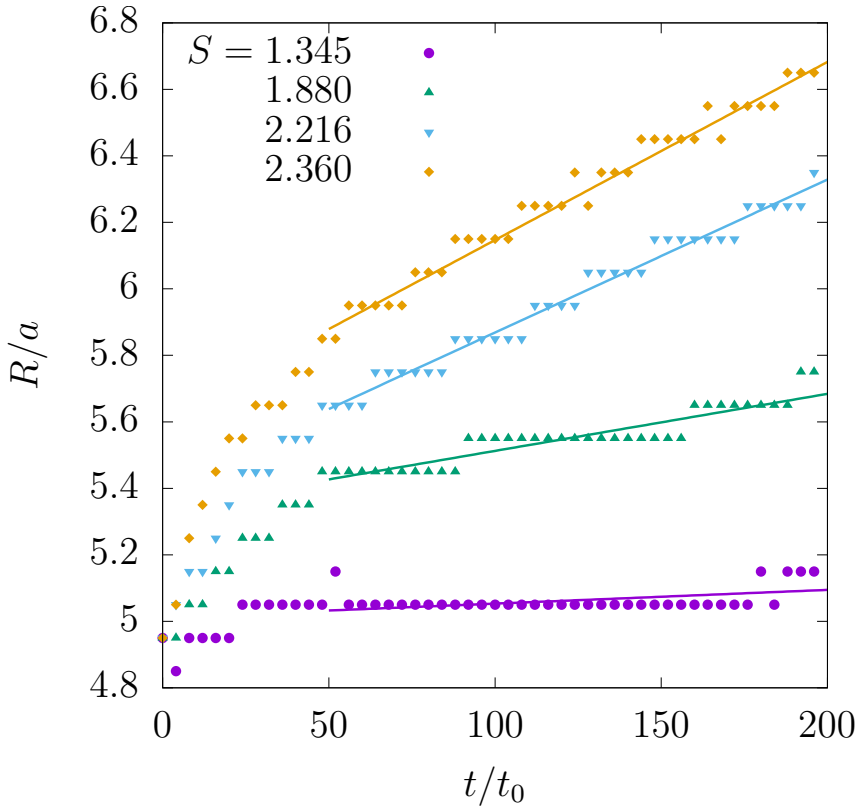

(a) Bulk temperature evolution

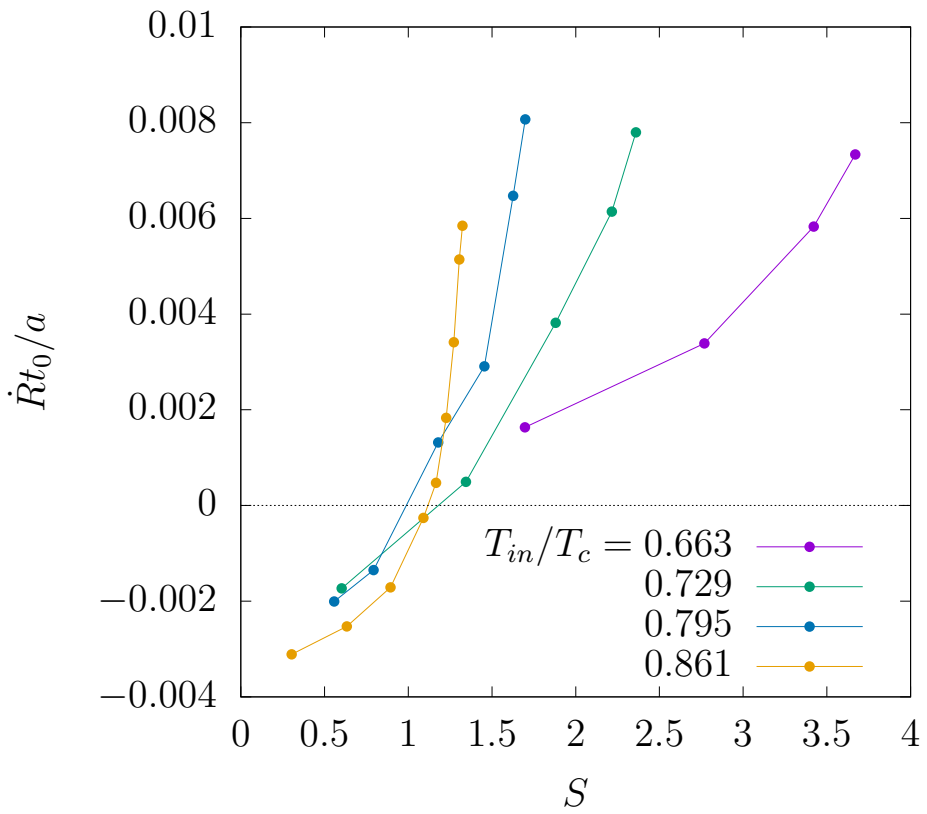

(b) Average droplet growth

Figure: (a) Typical growth curves for $T_0/T_c = 0.729$ and a series of supercooling ratios S, with the corresponding best linear fit lines. (b) Average droplet growth rate $\dot{R}$ with respect to the supercooling ratio $S = p(T, n_v)/p(T)$.

Growth of bubbles in superheated liquid - growth rate

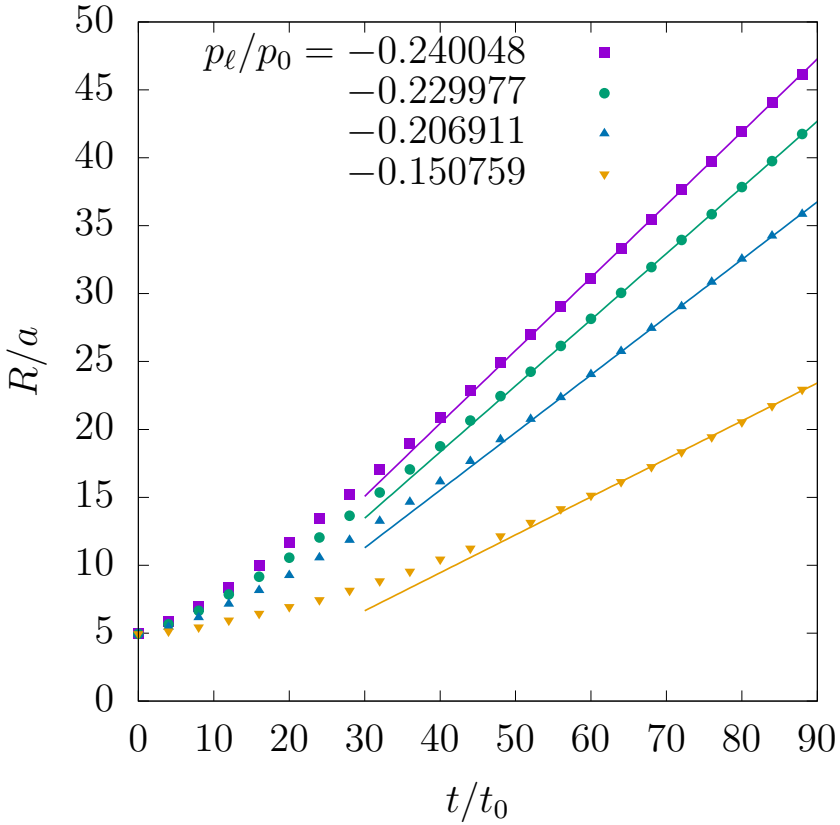

(a) $T_0/T_c = 0.663$

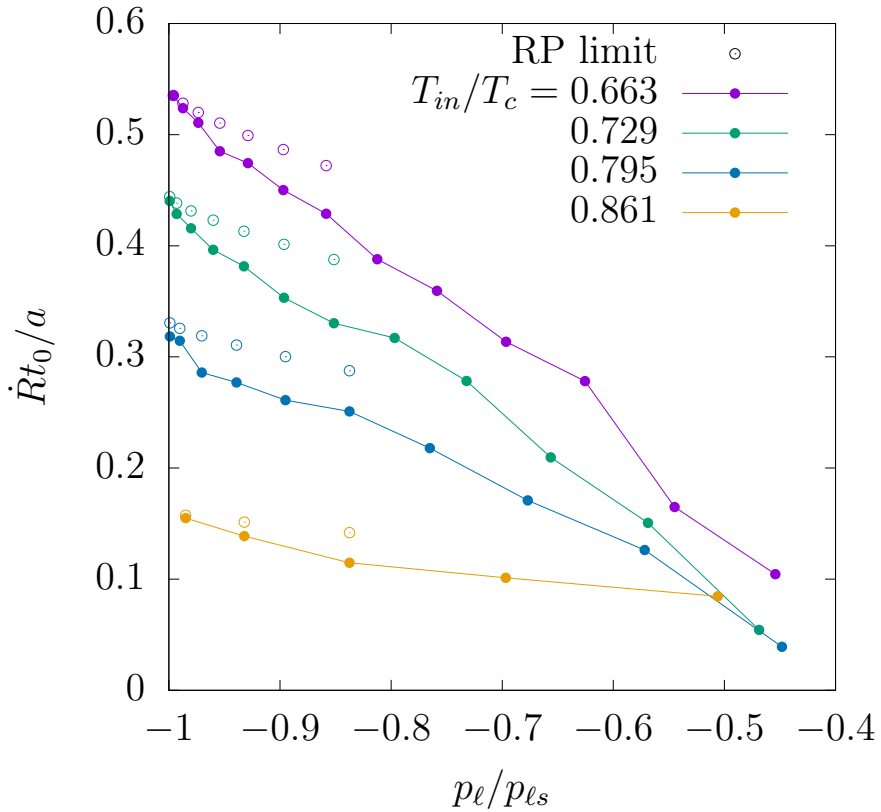

(b) Average bubble growth

Figure: (a) Typical growth curves for $T_0/T_c = 0.663$ and a series of liquid pressures p_ℓ with the corresponding best linear fit lines. (b) Average bubble growth rate $\dot{R}$ with respect to the surrounding liquid pressure $p_\ell/|p_{\ell s}|$, normalised to the value of the pressure on the spinodal line $p_{\ell s}$.

Growth of bubbles in superheated liquid - radial velocity

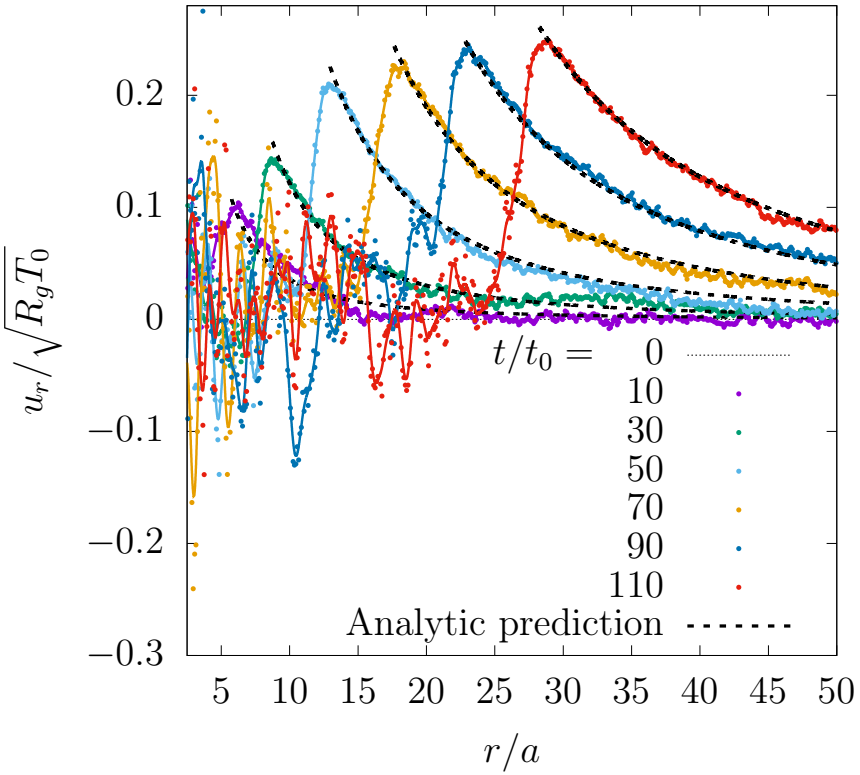

Radial macroscopic velocity profiles during bubble growth at $T_0/T_c = 0.729$ and $p_\ell = -0.1098$. The dashed analytic curves obtained following the model proposed by Vincent and Marmottant[5]:

$$u(r) = \frac{n_\ell - n_v}{(n_\ell - x^3 n_v)} \frac{x^2}{1 - x^3} \dot{R} \left[\frac{R_w^2}{r^2} - \frac{r}{R_w} \right], \quad \text{where } x = R/R_w \tag{13}$$

[5] O. Vincent and P. Marmottant, J. Fluid Mech. (2017), vol. 827, pp. 194–224

Growth of bubbles in superheated liquid - Temperature

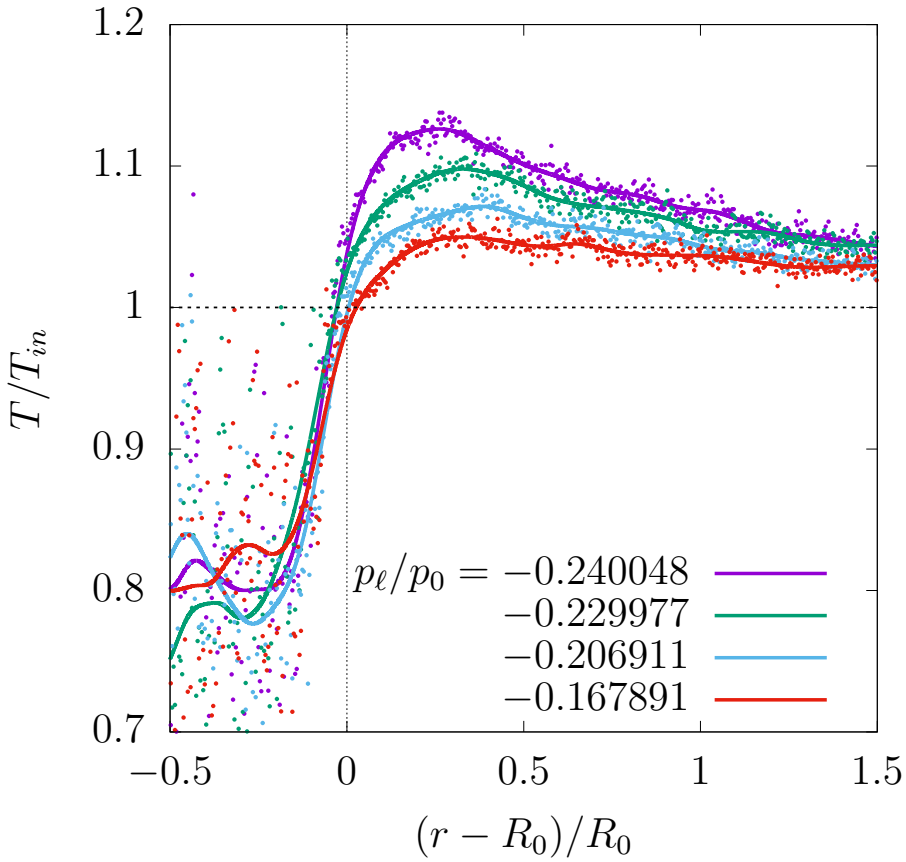

(a)

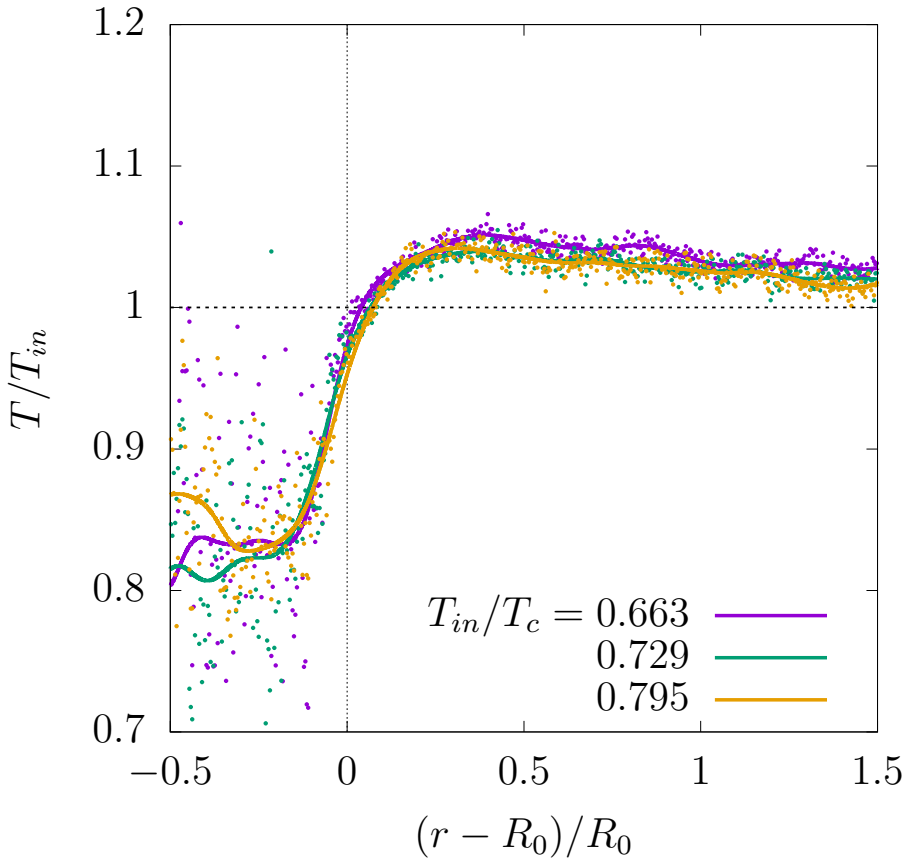

(b)

(a) Temperature profiles during bubble growth at $T_0/T_c = 0.663$ and $R_0 = 25a$.
(b) Temperature profiles during bubble growth at $\dot{R}t_0/a \approx 0.3$ and and $R_0 = 25a$.

Conclusions and outlook

- The EV equation is solved for the first time in spherical geometry using a weighted particle scheme. The collision dynamics between weighted particles has been derived accounting for the non-locality of the Enskog collision term, and a compact expression of the Vlasov mean force field has been determined using the shell theorem.
- Two benchmark cases were considered. First, and the numerical results were compared against the predictions of the Young-Laplace equation. Second, the critical radius of a droplet in its vapor was evaluated, and the numerical results were compared against the predictions of CNT. In both cases, an excellent agreement was found and this provided the validation of the numerical scheme.
- An extensive simulation campaign was then carried out to investigate the growth of droplets and bubbles in metastable vapor and superheated liquid, respectively.